Designing active sites for the sustainable low-temperature production of caprolactam using microporous zeotypes

M.E. Potter,[a] S. Chapman,[a] A .J. O'Malley,[b,c] A. Levy,[d~~b~~] M. Carravetta,[a] T. Mezza,[e~~c~~,e] S. F. ~~Parker~~[d]-Parker[f] and R. Raja[a]*

a) R.Raja@soton.ac.uk, Chemistry, University of Southampton, Highfield campus, Southampton, SO17 1BJ, UK.
b) UK Catalysis Hub, Research Complex at Harwell, Science and Technology Facilities Council Rutherford Appleton Laboratory, Harwell Science and Innovation Campus, Oxon OX11 0QX, UK.
c) Cardiff Catalysis Institute, School of Chemistry, Cardiff University, UK.
d~~b~~) Honeywell Int., 101 Columbia Road, Morristown, NJ 07962, USA.
e~~c~~) UOP LLC, 50 E. Algonquin Rd., Des Plaines, IL 60016, USA.
f~~d~~) ISIS Neutron and Muon Facility, Science and Technology Facilities Council Rutherford Appleton Laboratory, Harwell Science and Innovation Campus, Oxon OX11 0QX, UK.

Abstract

Modern society is placing increasing demands on commodity chemicals, driven by the ever-growing global population and the desire for improved standards of living. As the polymer industry grows, a sustainable route to ε-caprolactam, the precursor to the recyclable nylon-6 polymer, is becoming increasingly significant. To this end, we have optimised and characterised a recyclable SAPO catalyst using a range of characterisation techniques, to achieve near quantitative yields of ε-caprolactam from cyclohexanone oxime. The process is operated under significantly less energetically demanding conditions than any other industrial process to date.

Introduction

The nylon industry has been valued at 14 billion USD for 2019,[1,2] making the synthesis ε-caprolactam, the precursor for the recyclable Nylon-6 fibres, of great relevance. The two principle routes to caprolactam (the Raschig[3] and BASF[4] processes) achieve the acid-catalysed rearrangement of cyclohexanone oxime by using aggressive reagents, sacrificing sustainability for chemical activity. These undesirable practices can be circumvented by a vapour-phase process with a solid-acid catalyst[5] but the high temperatures required to keep both the lactam and oxime in the vapour-phase make this process energy intensive. Many catalysts have been investigated, but most suffer from the common drawbacks of high energy demands and limited catalyst stability.[6-12]

The liquid-phase Beckmann rearrangement employs lower temperatures, reducing energy consumption, typically at the cost of conversion.[13,14] As such, we recognise the demand for a catalyst that combines a single, targeted, catalytic site, with the selectivity of a nanoporous material. Aluminophosphates (AlPOs) are prime candidates, as their porous architectures offer high selectivity, akin to zeolites, while incorporating small quantities of dopants into an AlPO creates Brønsted acid sites, which vary in strength depending on the synthesis procedure and the topology of the framework.[15,16] A comparison of a range of silicon substituted AlPOs (SAPOs) and other porous structures emphasises the need for a carefully designed catalyst (Figure 1, Table S1). SAPO-37 shows great potential under these conditions, but a more general trend between pore size and activity is observed for the other SAPO materials. In contrast, although mesoporous MCM-41 offers little impedance to the diffusion of the organics, the material is less active than the SAPOs due to the lack of Brønsted acidity.[17,18]

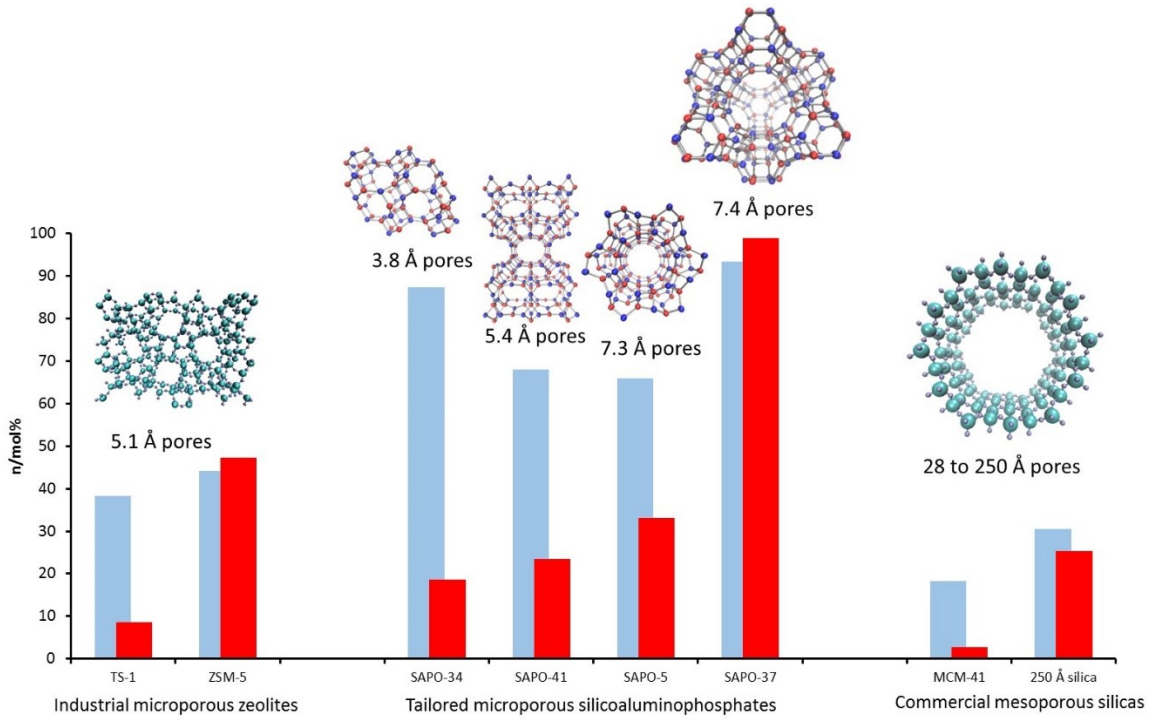

Figure 1. Comparing the catalytic activity of zeotypes. Conditions: 130 °C, catalyst: cyclohexanone oxime:benzonitrile ratio 1:1:200, 0.1 g of cyclohexanone oxime, 7 hrs. SAPO-37 here is SAPO-37(0.21).

MAS ^{29}Si NMR probed the silicon environments to explain the differing catalytic activity between the similar pore-sized SAPO-5 and SAPO-37. The ^{29}Si NMR spectrum of SAPO-37 shows a broad peak at -91 ppm (Figure S1), but cannot distinguish between $Si(OAl)_4$ and $Si(OAl)_3(OSi)$ due to the moisture-sensitivity of SAPO-37.[19] However, the peak position is still diagnostic of isomorphous substitution. In contrast SAPO-5 shows a broad peak centred at -101 ppm, indicative of silicon zoning to form $Si(OAl)_2(OSi)_2$, $Si(OAl)(OSi)_3$, $Si(OSi)_4$ species and extra framework sites.[19,20] This produces fewer, but stronger, Brønsted acid sites on the periphery of the silicon zones.[19,20] As such we propose that the isolated sites observed in the SAPO-37 system are active for this process, not the stronger acid sites on silicon islands.

To investigate the interactions between the SAPO-37 framework and cyclohexanone oxime Inelastic Neutron Scattering (INS) was employed. A scattering cross-section for neutrons means that INS spectra are dominated by vibrations associated with hydrogenous species, allowing the oxime and lactam to be probed in a physical mixture of 10% cyclohexanone oxime and 90% SAPO-37 (Figure 2). At 363 K the spectra clearly resemble that of the bulk oxime, while heating through a range of temperatures shows a progression to caprolactam, which is notable at 393 to 403 K, indicating that SAPO-37 has significant potential as a low-temperature, liquid-phase, Beckmann rearrangement catalyst.

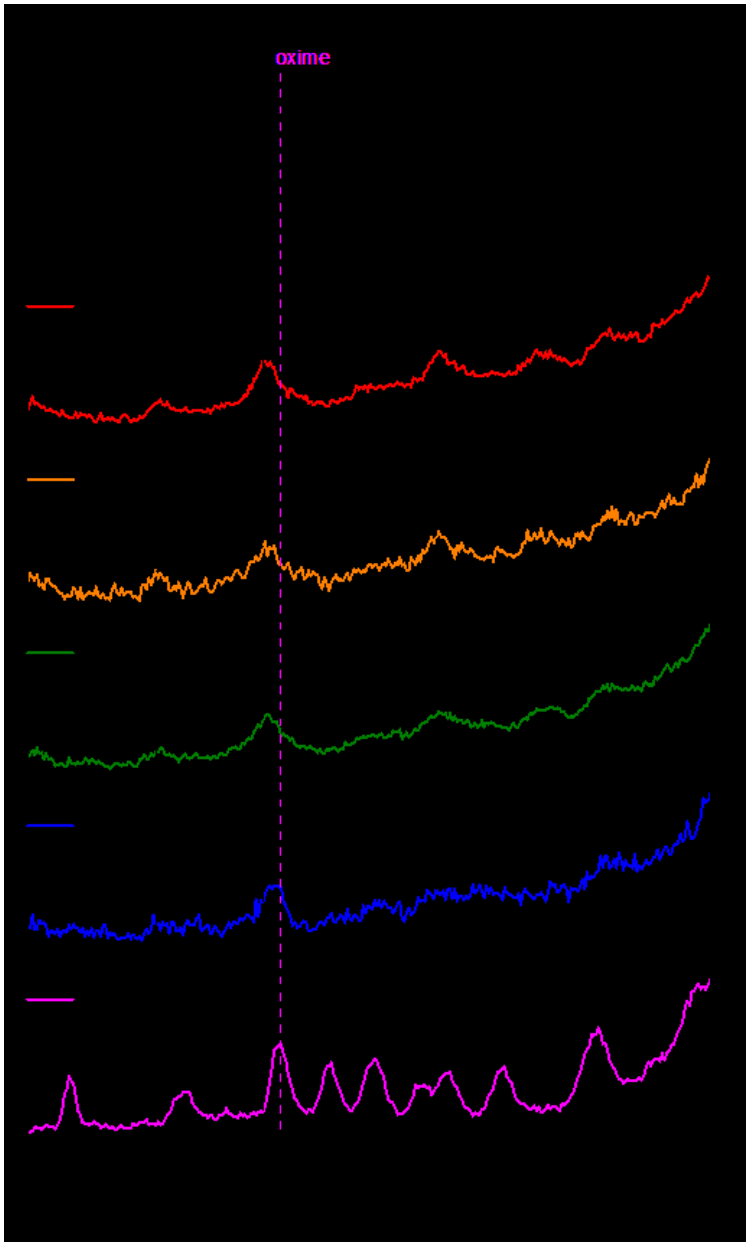

Figure 2. Variations in the vibrational spectrum (E_i = 100 meV) of a cyclohexanone oxime/SAPO-37 mixture on increasing temperature.

To optimise the SAPO-37 material, a range of silica-gel ratios were investigated (Table S9), labelled as SAPO-37(X), where X is the Si/P gel ratio. It was identified that an insufficient amount of silica in the synthesis promotes the formation of the more thermodynamically stable AFI phase. However SAPO-37(0.21), (0.42) and (0.63) showed similar powder-XRD patterns, confirming their crystallinity and phase-purity (Figure S2). Moreover, unit cell parameters were found to increase with increased silicon content, consistent with isomorphous subsitution.[20] The textural properties of the three SAPO-37 systems were in agreement with each other and literature values (Figures S3-S5).[21] 2D MAS ^{29}Si NMR showed the effect of silicon loading on the distribution of silicon environments (Figure 3A-C, Figures S1, S6 and S7). For increased resolution, experiments were performed under a constant flow of dry nitrogen for drive, purge and bearing. As a result, individual peaks at -98 and -93 ppm were resolved and assigned as $Si(OAl)_3(OSi)$ (from 5-silicon islands) and the isolated $Si(OAl)_4$ weak Brønsted acid species, respectively. The latter typically occurs between -89 and -92 ppm but the

nature of the experiment is believed to alter peak position. The spectra show that higher silicon loadings favour Si-O-Si bonding, through an increase in the -98 ppm signal; $(Si(OAl)_3(OSi)$,[20,22] relative to -93 ppm; $Si(OAl)_4$. Evidence for silicon clustering is seen at -101, -104 and -108 ppm in the SAPO-37(0.42) and (0.63) spectra, corresponding to $Si(OSi)_2(OAl)_2$, $Si(OSi)_3(OAl)$ and $Si(OSi)_4$ species, respectively, in both 1D and 2D NMR spectra.[19,20] These findings suggest that a lower silicon loading is necessary to promote the $Si(OAl)_4$ environment. Despite variations in the ^{29}Si NMR, both ^{27}Al and ^{31}P NMR signals were commensurate, showing predominantly $Al(OP)_4$ and $P(OAl)_4$ signals (Figures S9-S10).

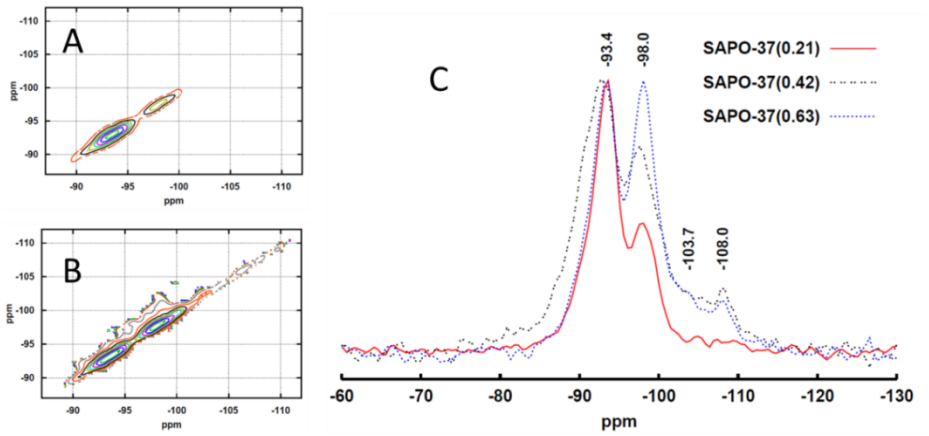

Figure 3. A) 2D MAS ^{29}Si NMR of SAPO-37(0.21). B) 2D MAS ^{29}Si NMR of SAPO-37(0.63). C) 1D MAS ^{29}Si NMR of SAPO-37 systems of different gel-ratios

Acid strength is key in the Beckmann rearrangement: active sites must be sufficiently strong to promote the formation of the lactam, yet weak enough to permit its desorption. TPD experiments show that SAPO-37(0.21) and (0.42) possess a similar number of acid sites (0.93 and 0.87 mmol/g respectively), though the SAPO-37(0.63) system had fewer (0.76 mmol/g, Figures 4 and Table S2). Lower silicon loadings favour a greater number of weaker acid sites (200-400 °C), whilst increasing the silicon loading promotes the formation of stronger acid sites (400-500 °C). These observations reinforce the NMR findings.[23-25] The TPD values obtained for the SAPO-37(0.21) also correlate well with the theoretical total acidity, (Schemes S1 and S2, Table S3 and S4) calculated from the ICP and NMR (0.98 mmol/g).

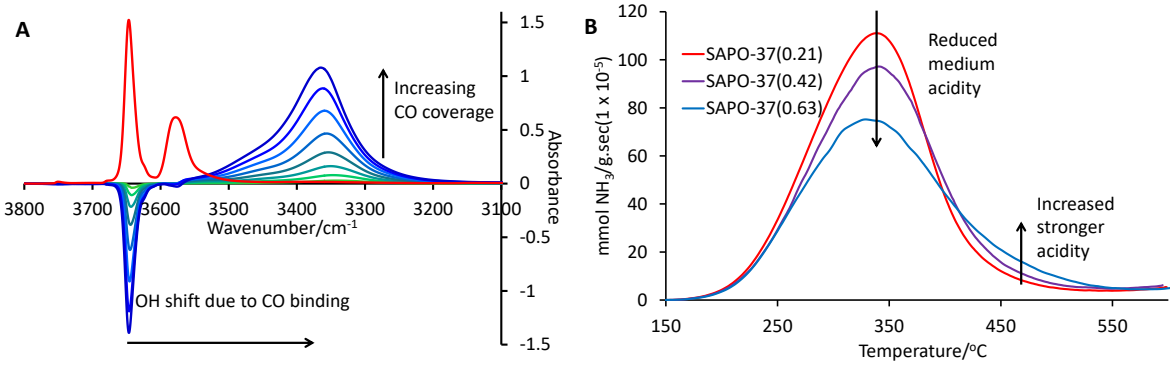

Figure 4. A) The influence of CO binding on the hydroxyl region of SAPO-37(0.21) while B) NH_3-TPD data which reveals a greater quantity of strong acid sites in higher loading SAPO-37 species.

The FT-IR spectra of SAPO-37 show bands at 3641 and 3575 cm^{-1} corresponding to the hydroxyls in the supercage and sodalite cages of the faujasitic framework, respectively (Figure 4 and Figure S11). A comparable intensity of the 3641 cm^{-1} band shows that SAPO-37(0.21) and (0.42) possess similar quantities of hydroxyl groups, but more than SAPO-37(0.63) (Figure S12-S14, Table S5). Low temperature CO adsorption showed only the 3641 cm^{-1} band, which was reduced significantly as a new band appeared at 3330 cm^{-1}, confirming interaction with the CO. The inflection at 3450 cm^{-1} is attributed to CO interacting with P-OH bonds, and proton migration. The magnitude of the hydroxyl band shift on CO adsorption is linked to the average acid strength of the material, which also increased with silicon loading, in agreement with TPD data (Figure S11-S14, Table S5). The CO band at 2180-2160 cm^{-1}, which can be used to quantify total acidity, highlights the similarities between SAPO-37(0.21) and (0.42), in contrast to SAPO-37(0.63) which possesses fewer acid sites. From this data, the proton affinity was calculated as 1155, 1152 and 1146 kJ mol^{-1} for SAPO-37(0.21), (0.42) and (0.63), respectively,[26] in agreement with literature values.[27] Collidine was used as a similar-sized probe to cyclohexanone oxime, giving information on accessibility. The 1652 and 1637 cm^{-1} bands (O-H···N interactions, Figures S15-S18, Table S6), were quantified at different temperatures to probe acid strength. This data ratifies the observation that a lower silicon content favours more weak acid sites. Using a variety of characterisation techniques we have shown that SAPOs with comparable physical characteristics can be prepared, and that by reducing silicon content, it is possible to promote the formation of isolated, weak acid sites that are suitable for the Beckmann rearrangement.

In the liquid-phase Beckmann rearrangement, variations in lactam yield between the different SAPO-37 species are apparent (Table 1, S7, and Figures S19-S42). As SAPO-37(0.21) and (0.42) possess a similar quantity of acid sites, the improved selectivity for caprolactam at lower silicon loading is attributed to the targeted weaker acid sites (Table 1). These weaker acid sites enable faster lactam desorption, therefore, SAPO-37(0.21) can produce caprolactam at a faster rate (Table 1). Above 170 °C, temperature was found to have little effect on the reaction rate, suggesting the process becomes limited by mass-transfer (Table S7). Arrhenius analysis verified that the production of caprolactam is first-order reaction, in agreement with the mechanism postulated for the Beckmann rearrangement.[26] SAPO-37(0.21) is associated with a lower activation energy (Figure S43, Table S8) which, at 50 kJ mol^{-1}, in good agreement with work performed for the vapour-phase,[28] (Scheme S3) suggesting that the reaction proceeds via an analogous pathway in the liquid-phase.

Table 1. Summary of catalytic results for the low-temperature Beckmann rearrangement of cyclohexanone oxime to ε-caprolactam.

System	Time/mins	Conversion/mol%	ε-caprolactam selectivity/mol%[a]	Total Acid quantity/(mmol/g)[b]	Degree of site isolation/%[c]	Weak + Medium acid sites/(au/mg)[d]
SAPO-37(0.21)	180	93.4	97.8	0.93	71	3.76
Anhydrous	420	99.8	97.8			
SAPO-37(0.21)	180	89.3	96.0	0.93	71	3.76
Wet	420	98.9	93.5			
SAPO-37(0.42)	180	89.8	93.3	0.87	48	3.11
Wet	420	98.8	90.3			
SAPO-37(0.63)	180	90.4	90.9	0.77	41	2.80
Wet	420	99.8	88.4			

Conditions as per Figure 1. a) Other products include cyclohexanone and products arising from solvent-oxime interactions. b) Taken form NH_3-TPD. c) As determined by curve fitting ^{29}Si MAS NMR. d) As per collidine FT-IR.

As water promotes site deactivation and cyclohexanone production,[29] the Beckmann rearrangement was optimised under anhydrous conditions (Table 2, Figure S44-S47) to improve conversion and selectivity (Table 1 and Table S9) to near-quantitative yield of ε-caprolactam. A range of anhydrous solvents were tested, but only benzonitrile and chlorobenzene offered significant enhancements. This has been attributed to the presence of a polar-group attached to a non-polar ring, allowing for good miscibility with both reactants and products, at a high boiling point (Figure S48). We further confirmed the heterogeneous nature of the catalyst; showing the catalytic activity of the material was retained on reactivation (Figure S49).

In conclusion the work represents a significant advancement towards understanding how achieving industrially attractive yields of ε-caprolactam can be achieved *via* a liquid-phase Beckmann rearrangement. Systematic control of synthesis parameters can be used to control the acidity of SAPO materials. Furthermore, we are able to demonstrate, through the use of catalytic and spectroscopic analyses, the relationship between the nature and strength of acidic active sites and catalytic efficiency (Table 1), to achieve near-quantitative yield of caprolactam.

References

1. "Nylon – A global strategic business report" Global industry analysts inc., **2010**
2. "World analysis – Nylon engineering resins" IHS chemicals, http://www.ihs.com/products/chemical/planning/world-petro-analysis/nylon-engineering-resins.aspx
3. Bellussi, G.; Perego, C. *CATTECH*, **2000**, 4, 4-16
4. Holderich, W.F.; Roseler, J.; Heitmann, G.; Liebens, A.T. *Catal. Today.*, **1997**, 37, 353-366
5. Izumi, Y.; Ichihashi, H.; Shimazu, Y.; Kitamura, M.; Sato, H. *Bull. Chem. Soc. Jpn.*, **2007**, 80, 1280-1287
6. Sharghi, H.; Sarvari, M.H.; *J. Chem. Res.,* **2003**, *3*, 176
7. Curtin, T.; McMonagle, J.B.; Hodnett, B.K.; *Appl. Catal. A. Gen.,* **1992**, *93*, 91-101
8. Anilkumar, M.; Hoelderich, W.F. *J. Catal.,* **2008**, *260*, 17-29
9. Kob, N.; Drago, R.S. *Catal. Lett.,* **1997**, *49*, 229-234
10. Zhang, Z.; Li, J.; Yang, X. *Catal. Lett.,* **2007**, *118*, 300-305
11. Shiju, N.R.; Anilkumar, M.; Holdereich, W.F.; Brown, D.R. *J. Phys. Chem. C.*, **2009**, 113, 7735-7742
12. Hetimann, G.P.; Dahlhoff, G.; Holderich, W.F. *Appl. Catal. A. Gen.*, **1999**, 185, 99-108
13. Camblor, M.A.; Corma, A.; Garcia, H.; Semmer-Herledan, V.; Valencia, S. *J. Catal.*, **1998**, 177, 267-272
14. Ngamcharussrivichai, C.; Wu, P.; Tatsumi, T. *Appl. Catal. A. Gen.,* **2005**, 288, 158-168
15. Thomas, J.M.; Raja, R.; Sankar, G.; Bell, R.G. *Nature*, **1999**, 398, 227-230
16. Barrett, P.A.; Sankar, G.; Catlow, C.R.A.; Thomas, J.M. *J. Phys. Chem.*, **1996**, 100, 8977-8985
17. Jentys, A.; Pham, N.G.; Vinek, H. *J. Chem. Soc. Faraday Trans.,* **1996**, 92, 3287-3291
18. Chen, J.; Li, Q.; Xu, R.; Xiao, F. *Angew. Chem. Int. Ed.,* **1995**, 34, 2694-2696
19. Blackwell, C.S.; Patton, R.L. *J. Phys. Chem.*, **1988**, 92, 3965-3970
20. Potter, M. E.; Cholerton, M. E.; Kezina, J.; Bounds, R.; Carravetta, M.; Manzoli, M.; Gianotti, E.; Lefenfeld, M.; Raja, R. *ACS Catal.* **2014**, 4, 4161-4169.
21. Mostad, H.B.; Stocker, M.; Karlsson, A.; Rorvik, T. *Appl. Catal. A: Gen.*, **1996**, 144, 305-317
22. Peltre, M.J.; Man, P.P.; Briend, M.; Derewinski, M.; Barthomeuf, D. *Catal. Lett.*, **1992**, 16, 123-128
23. Wendelbo, R.: Akporiaye, D.; Andersen, A.; Dahl, I.M.; Mostad, H.B. *Appl. Catal. A:Gen.*, **1996**, 142, L197-L207
24. Lee, Y-J.; Baek, S-C.; Jun, K-W. *Appl. Catal. A:Gen*, **2007**, 329, 130-136
25. Sastre, G.; Lewis, D.W.; Catlow, C.R.A. *J. Phys. Chem. B.*, **1997**, 101, 5249-5262
26. Reddy Marthala, V.R.; Jiang, Y.; Huang, J.; Wang, W.; Glaser, R.; Hunger, M. *J. Am. Chem. Soc.*, **2006**, 128, 14812-14813.
27. Coluccia, S.; Marchese, L.; Martra, G. *Micro. Meso. Mater.,* **1999**, 30, 43-56
28. Bucko, T.; Hafner, J.; Benco, L. *J. Phys. Chem. A*, **2004**, 108, 11388-11397

29. Ngamcharussrivichai, C.; Wu, P.; Tatsumi, T. *J. Catal.*, **2005**, 235, 139-149